Eddy Formation by Overflows in Stratified Water

GREGORY F. LANE-SERFF

School of Ocean and Earth Science, University of Southampton, Southampton Oceanography Centre, Southampton, United Kingdom

PETER G. BAINES

CSIRO Atmospheric Research, Aspendale, Victoria, Australia

(Manuscript received 3 August 1998, in final form 16 March 1999)

ABSTRACT

The formation of eddies by dense overflows in stratified water is examined by laboratory experiments. The dense fluid initially flows down the slope but turns (under the influence of rotation) to flow along the slope. The inviscid alongslope flow is continuously drained by a viscous Ekman layer that flows more directly downslope. In some cases this Ekman layer flow becomes unstable to growing waves. Under certain conditions, strong cyclonic vortices form in the ambient fluid above the alongslope flow due to vortex stretching, causing the dense fluid to break up into a series of domes. There are three main mechanisms for this: first, the initial downslope flow of the current (before it turns under the influence of rotation) may take ''captured'' upper-layer fluid with it out into deeper water; second, adjustment of the current to geostrophic balance stretches the fluid column above the current; and, finally, the continuous viscous draining from the current (and later from the domes) also causes stretching in the ambient fluid.

The vertical extent of the influence of the overflow (and thus the initial effective height of these columns of ambient fluid) is controlled by the stratification in the ambient fluid. Two types of stratification are examined: a two-layer ambient fluid with an interface above the overflow and a linearly stratified ambient fluid. For the two-layer ambient fluid the relevant vertical scale is simply the height of the interface above the overflow, d_I, while for the linearly stratified case a height scale based on the strength of the stratification is derived, d_N. The stretching of the columns of ambient fluid is measured by the parameter $\Gamma_I = L\alpha/d_I$ or $\Gamma_N = L\alpha/d_N$, where L is the Rossby deformation radius and α is the bottom slope. The frequency at which the eddy/dome structures are produced increases with the stretching parameter Γ, while the speed at which the structures propagate along the slope depends on viscous effects. The behavior is very similar to that for flow into an unstratified ambient fluid where the stretching parameter $\Gamma = L\alpha/D$, where D is the total fluid depth, except that the propagation speed of the eddies along the slope is slower in the stratified case by a factor of approximately 0.7. The flow of dense fluid on slopes is a very important part of the global ocean circulation system, and the implications of the laboratory experiments for oceanographic flows are discussed particularly for Denmark Strait.

1. Introduction

The flow of dense water from marginal seas or through sills down into the deep ocean is an important part of the global thermohaline circulation. Examples include the flow of dense water formed by cooling in the polar oceans and high salinity flows from evaporative marginal seas such as the Mediterranean and the Red Sea. These dense flows do not generally descend directly down the continental slope into the deep ocean but flow along the slope under the influence of the earth's rotation, with a gradual draining into the deep ocean. Strong cyclonic vortices have been observed in connection with overflow currents, especially downstream of the Denmark Strait (Bruce 1995; Krauss 1996).

In a review of convection in geophysical systems, Maxworthy (1997) identified the flow of dense fluid down slopes as an important class of flow that had received limited attention in the laboratory. Zatsepin et al. (1998) made laboratory models of flows generated by a source on a conical slope. However, that work concentrates on cases where (nearly) barotropic anticyclonic vortices are generated by injecting source fluid of equal or only slightly greater density than the ambient fluid. Observations of eddy formation by downslope flows in homogeneous environments have also been described by Condie (1995) and Etling (1997; 1998, personal communication).

In our recent paper (Lane-Serff and Baines 1998,

Corresponding author address: Dr. Gregory F. Lane-Serff, School of Ocean and Earth Science, University of Southampton, Southampton Oceanography Centre, European Way, Southampton SO14 3ZH, United Kingdom.
E-mail: G.F.Lane-Serff@soton.ac.uk

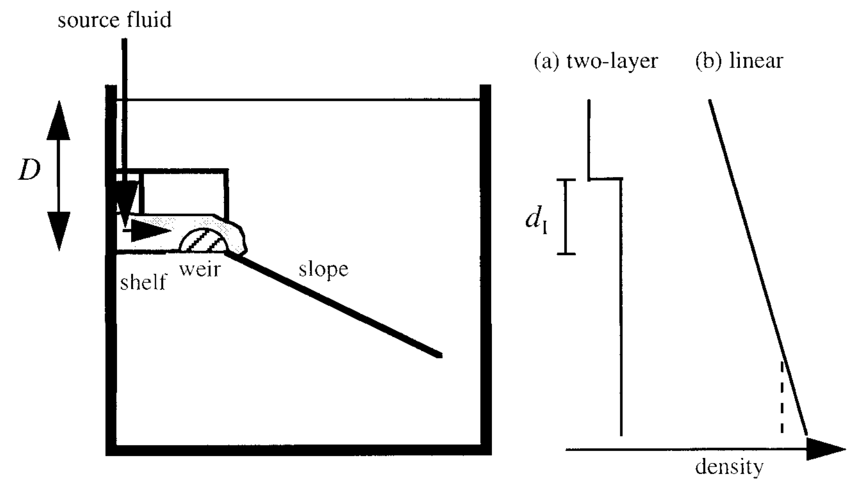

FIG. 1. Schematic cross section of the apparatus. Also shown are the two types of stratification used: (a) two-layer and (b) linearly stratified. In practice the density below the bottom of the slope was usually uniform (as shown by the dashed line).

hereafter denoted LSB), we examined the complex behavior of this type of flow by making laboratory experiments and described the conditions under which the dense current can generate these strong cyclonic vortices (or eddies) in the overlying fluid. We showed how the eddies were created by stretching the vorticity in the ambient fluid as the dense current took overlying fluid out into deeper water before turning to flow along the slope. Once established, some distance from the source, the flow can be regarded as having two main components: an inviscid alongslope flow and a viscous, draining, downslope flow.

In LSB we restricted attention to flows where the ambient fluid was of uniform density. We now consider the more realistic case where the ambient fluid is stratified. Two types of stratification are considered (Fig. 1). The first is a two-layer system with the interface some distance above the source of dense water. This simulates, for example, a flow in which a strong thermocline is the most significant feature of the ambient stratification. The second is a uniformly linearly stratified ambient water column. In this second case the dense fluid will eventually reach a level of neutral density and leave the slope. While the injection of the dense fluid into the water column as it leaves the slope is very important it is beyond the scope of the present work, and will be examined in later studies.

For the unstratified case the creation of cyclonic vortices depends on stretching columns of ambient fluid that extend from the top of the dense current up to the surface. The strength and frequency of the eddies depends on the relative amount of stretching so that the eddies are stronger and more frequent in shallower water. In stratified water the vertical extent of fluid motions in the ambient fluid associated with the overflow is limited by the stratification. This enhances the relative stretching of columns of ambient fluid and thus we expect overflows in stratified water to cause stronger and more frequent eddies than in unstratified water.

In the next section we discuss the scalings appropriate to this problem. Those scales that relate to an unstratified ambient fluid are discussed in detail in LSB, and we cover them more briefly here. A total of 20 experiments were conducted with a range of slopes, ambient stratification, and other parameters. In section 3 the apparatus and the experimental parameters are described. The results are given in section 4, and these results and their oceanographic implications and relation to other works on overflows are discussed in the final section.

2. Scalings

a. *Unstratified ambient fluid*

The parameters that are set externally are the density of the inflow, the flow rate, and the rotation. We use g' to denote the reduced gravity $g' = (\Delta\rho/\rho)g$, where the density difference between the source fluid and the local ambient fluid (at the level of the source) is used. The Coriolis parameter is denoted by f and the flow rate by Q. The flow adjusts so that its width scales on the Rossby deformation radius L. This gives our estimates of the appropriate height and width scales for the dense current,

$$d = \sqrt{(2Qf/g')}, \tag{1a}$$

$$L = (2Qg')^{1/4} f^{-3/4}, \tag{1b}$$

with the alongslope velocity in the current,

$$u = (2Qfg')^{1/4}. \tag{2}$$

If an isolated volume of dense fluid is moving along the slope (with uphill being to the left in the Southern Hemisphere) the Coriolis acceleration will be upslope while the gravitational acceleration will be downslope.

The alongslope speed for which these accelerations balance is given by

$$c_N = g'\alpha/f, \quad (3)$$

where α is the (small) angle of the slope from the horizontal. This speed is also known as the Nof speed (e.g., Swaters and Flierl 1991).

The thickness of the viscous draining layer scales on the Ekman layer thickness,

$$d_\nu = \sqrt{2\nu/f}, \quad (4)$$

where ν is the kinematic viscosity (taken here to be 0.01 $cm^2\ s^{-1}$). The velocity in this layer scales on c_N (see Nagata et al. 1993), thus we can introduce an alongslope length scale that relates to the distance over which the initial flux is drained,

$$Y = (Qf^{3/2})/(g'\alpha\sqrt{2\nu}). \quad (5)$$

We expect viscous effects to be unimportant at distances short compared with Y, but to become significant at distances of order Y and larger. The relative importance of the viscous draining can be quantified in terms of the ratio of the alongslope draining distance to the width of the flow,

$$Y/L = 2^{-3/4}Q^{3/4}f^{9/4}\nu^{-1/2}g'^{-5/4}\alpha^{-1}. \quad (6)$$

The current initially flows downslope a distance that scales on the Rossby radius before it turns and flows alongslope. In both laboratory and numerical models the dense flow is observed to ''drag'' the overlying fluid with it (for more discussion see sec. 5). If we assume that the current takes the ambient fluid above it out into deeper water, then we see that the ambient fluid is stretched by an amount of order $L\alpha$. This, compared with the initial height of the ambient fluid columns, gives the relative stretching as

$$\Gamma = L\alpha/D, \quad (7)$$

where D is the depth of the ambient fluid above the incoming current.

In LSB we showed that eddies were formed in the ambient fluid above the dense current provided that there was sufficient vortex stretching and provided that the viscous draining was not too strong ($\Gamma > 0.07$ and $Y/L > 3.5$ for our experiments). The frequency of the eddies increased with Γ, while the speed at which the eddies propagated depended on the viscous draining (with the speed increasing with Y/L).

b. Stratified ambient fluid

We now turn our attention to the effects of stratification in the ambient fluid on the flow. Two cases are considered: first, a simple two-layer stratification and, second, a linearly stratified ambient fluid. In the two-layer case the interface between the two layers (if strong enough) provides an obvious upper boundary to the flow. Thus we use a similar stretching parameter to that used in the unstratified case, simply substituting the height of the interface above the incoming fluid, d_I for the total depth D,

$$\Gamma_I = L\alpha/d_I. \quad (8)$$

We define the relative strength of the stratification in terms of the density difference between the incoming fluid and the local ambient fluid,

$$r = (\rho_L - \rho_U)/(\rho_S - \rho_L), \quad (9)$$

where ρ_L and ρ_U are the densities of the initial upper and lower layers, respectively, and ρ_S is the density of the source fluid.

For the linearly stratified case, we can define an associated height scale,

$$d_N = Lf/N = (2Qfg')^{1/4}N^{-1}, \quad (10)$$

where N is the buoyancy frequency of the ambient fluid. This height is the vertical scale over which we expect the motion in the ambient fluid to decay, though the decay will be gradual as distinct from the more abrupt change at the interface in the two-layer case. We can then define a stretching parameter based on this height scale,

$$\Gamma_N = L\alpha/d_N = N\alpha/f. \quad (11)$$

Note that this is independent of the source conditions (though in practice it is necessary to check that d_N is smaller than D, else the stratification would not be significant). We can calculate a relative stratification in a similar way as for the two-layer cases: using the local ambient density in place of the lower-layer density and the density at height d_N for the upper-layer density. This gives the relative stratification as

$$r = (2Qf)^{1/4}Ng'^{-3/4} = d/d_N, \quad (12)$$

so the relative stratification is equal to the ratio of the current thickness to the stratification height scale. Thus r is also the relevant parameter for describing how the stratification affects the current itself.

3. Experiments

The experimental details are similar to those described in LSB. The experiments were conducted in a square glass tank (base 75 cm × 75 cm, height 70 cm) or a circular perspex tank (diameter 95 cm, height 50 cm) mounted on a rotating table. Simple plane slopes (angles 5.7° and 15.7° from the horizontal) were used in the square tank, while a truncated cone (angle 13.8°) was used in the circular tank. The dense source fluid was introduced via a gravity feed into a channel on a shelf at the top of the slope. From there it flowed over a weir onto the slope, flowing initially directly down the slope (Fig. 1).

The procedure for filling the tanks with stratified fluid was as follows. For the two-layer case the tank was filled with the required volume of freshwater (for the

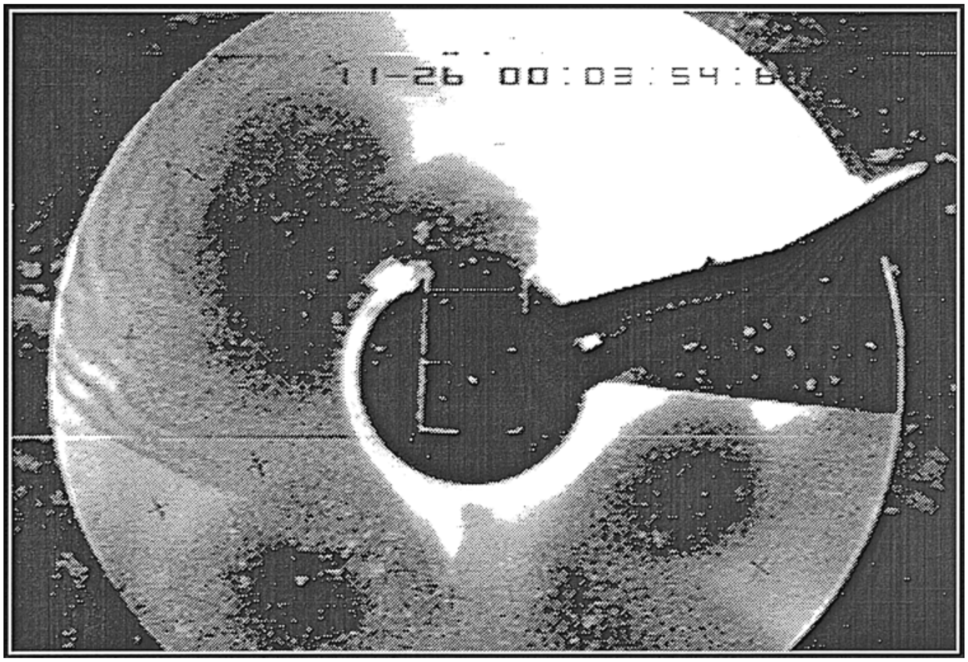

FIG. 2. A plan view of an experiment in the circular tank showing a series of dense domes moving around the conical hill. The parameters are $g' = 23.9$ cm s^{-2}, $Q = 25$ cm^3 s^{-1}, $d_l = 10$ cm (two-layer ambient fluid), and rotation rate of one revolution in 6.0 s.

upper layer) and then the tank was rotated until the water had reached solid body rotation (approximately 20 minutes). A denser lower layer (brine) was then added slowly underneath the upper layer while the tank was rotating. The density structure was monitored during the filling process by extracting samples via a fixed tube (fixed some 20–30 cm above the base of the tank). The interface thickness (in which at least 95% of the density change occurred) was generally in the range 2 to 3 cm. To produce a linearly stratified environment a two-bucket system was used, with the tank rotating throughout the filling process. For this case a uniform dense layer was usually added below the stratified fluid, with this dense layer extending no higher than the base of the slope. The depth of ambient fluid above the source was between 20 and 35 cm.

The source fluid was always denser than any of the ambient fluid so that, once it left the slope, it could cascade to the bottom of the tank and not interfere with the later flow. For the linearly stratified case, however, mixing with the ambient fluid did produce some fluid that did not descend to the bottom of the tank, apparently due to the detrainment process described by Baines (1998). Values of g' (based on the density difference between the source fluid and the local ambient fluid at shelf height) ranged from 5 to 100 cm s^{-2}, while source flow rates were approximately 25 cm^3 s^{-1} for all cases. The rotation period was between 6 and 12 seconds, giving f between 1 and 2 s^{-1}. The values of the height scales (d_l and d_N for the two-layer and linearly stratified cases, respectively) varied between 3 and 15 cm.

The parameters were chosen so that eddies would not be expected in the absence of stratification, based on our unstratified experiments in the same tanks (all of the experiments have $Y/L < 3$ or $\Gamma < 0.06$). For most of the experiments the dense fluid was dyed and the flow filmed from above using a video camera mounted on the rotating table superstructure. A video image from one of the experiments in the circular tank is shown in Fig. 2.

For two experiments the fluid was marked with particles instead of dye to recover more accurate velocity information. The particles used were small polystyrene beads with densities in the range 1.00 to 1.03 g cm^{-3}; in one of these experiments particles (of diameter 0.2 mm) were mixed into the source fluid, while in the other the particles (of diameter 1.0 to 1.4 mm) were placed in the ambient fluid. For the particle experiments the experiment was illuminated with sheets of light. For the first experiment the light sheet was parallel to the slope and approximately 3–5 mm above the slope. In the second experiment horizontal sheets of light were used. The light sheet was moved during the course of the experiment to illuminate the level of the top of the slope and then at 5 cm, 10 cm, and 15 cm above the top of the slope.

4. Results

The parameter space covered by the experiments is shown in Fig. 3. For this figure a stretching parameter based on the relevant stratified height scale is used (i.e.,

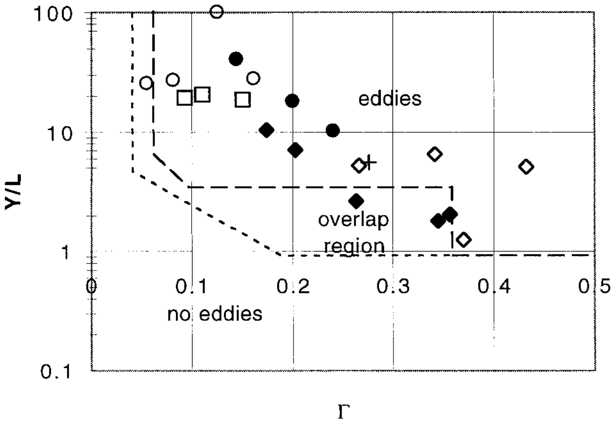

FIG. 3. The parameter space covered by the experiments. The subdivision of the parameter space is from *unstratified* experiments (LSB). Eddies were observed in most of the experiments, the exceptions being three in the ''overlap'' region and one just inside the ''eddies'' region, all having $Y/L < 4$. See Fig. 7 for definition of symbols.

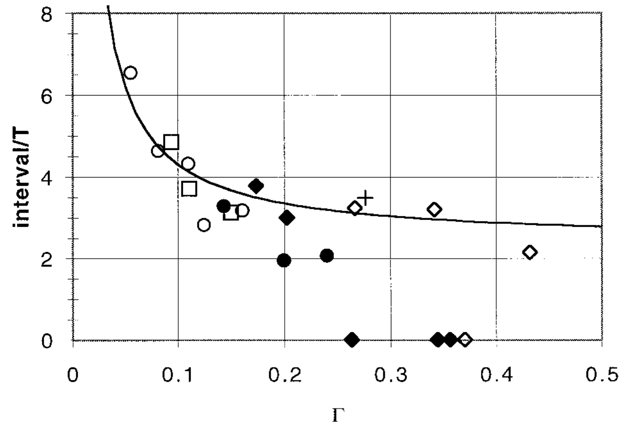

FIG. 4. The interval between one eddy and the next as a function of the stretching parameter (Γ_I or Γ_N) based on the relevant height scale.

Γ_I for two-layer stratification, Γ_N for linear stratification). The parameter space is divided into regions based on the *unstratified* results from LSB. For the present experiments eddies were observed in all but four of the experiments: the three in the ''overlap region'' and one just within the ''eddies'' region.

The variation of the frequency of the eddies with stretching is shown in Fig. 4 (in terms of the time interval between one eddy and the next, T_{int}), along with the best-fit line from the unstratified experiments ($T_{int}/T = 0.19/\Gamma + 2.4$). Both types of stratification give results that do not differ significantly from the unstratified case if the fluid depth is replaced with the appropriate vertical scale. It is, perhaps, not surprising that the interface imposes a ''lid'' on the flow in the two-layer case. Strong cyclones were observed in the ambient lower layer above the domes of dense fluid, and these cyclones were accompanied by a depression in the interface. It is not so clear, a priori, that a similar effect would occur for the continuously stratified case. We expected the vertical extent of the motion to be limited by the stratification, but were not necessarily expecting the effect to be so similar to a simple interface. Furthermore, even if the effect is similar, we did not necessarily expect the relevant vertical scale to be exactly d_N: the appropriate scale might have been d_N multiplied by some constant. From our results it appears that this constant is not significantly different from unity, but this must be regarded as fortuitous.

The fluid velocities were measured in the particle experiments using the particle tracking routines in DigImage. For each velocity calculation 15 images were digitized at intervals of 0.08 s, and a mean velocity for the total period (1.12 s) calculated. Typical velocity and vorticity fields in the dense source layer are shown in Fig. 5, while those at various levels in the ambient fluid are shown in Fig. 6. Strong cyclonic vortices are visible in the dense layer, in the horizontal layer, level with the top of the slope, and in the layer 5 cm above that (peak vorticities of approximately $1.1f$, $0.45f$, and $0.4f$, respectively). Given the slope and the location of the eddies, the horizontal light sheets are approximately 3 cm and 8 cm above the slope at the eddy positions (0.5 and $1.2d_N$). In the light sheets above these (i.e., at 10 cm and 15 cm) there is a slow, secondary anticyclonic motion that appears to occupy the full extent of the tank, presumably driven by the dense fluid cascading off the slope and generating motion on the scale of the tank, but no apparent motion associated directly with the eddies. Thus the influence of the dense fluid on the ambient fluid is limited in vertical extent, decaying on a vertical lengthscale of order d_N.

Turning our attention to the motion of the eddies as a whole (rather than the fluid velocity within them), the speed of propagation of the dome/eddy structures appears to depend on the importance of viscous effects and is given by $(0.067 \pm 0.002)c_N(Y/L)^{0.62}$ for both the two-layer and continuously stratified cases (where we have kept the same power law as the best fit for the unstratified case, and only varied the multiplicative constant). This is slower than for the unstratified case by a factor of approximately 0.7 (Fig. 7). This may be due to the generation of interfacial or internal waves, and is worthy of further study.

The relative stratification [as defined in Eqs. (9) and (12)] does not appear to be very significant (Fig. 8), with eddies produced even when this is small (down to 0.25). In practice there must be a lower limit below which the stratification does not have a significant effect on the flow. For the two-layer case this is likely to be when the eddies produce depressions in the interface comparable with the depth of the lower layer, while for the linearly stratified case the height scale d_N can only be important so long as it is no larger than the total depth D (d_N increases as the stratification becomes weaker).

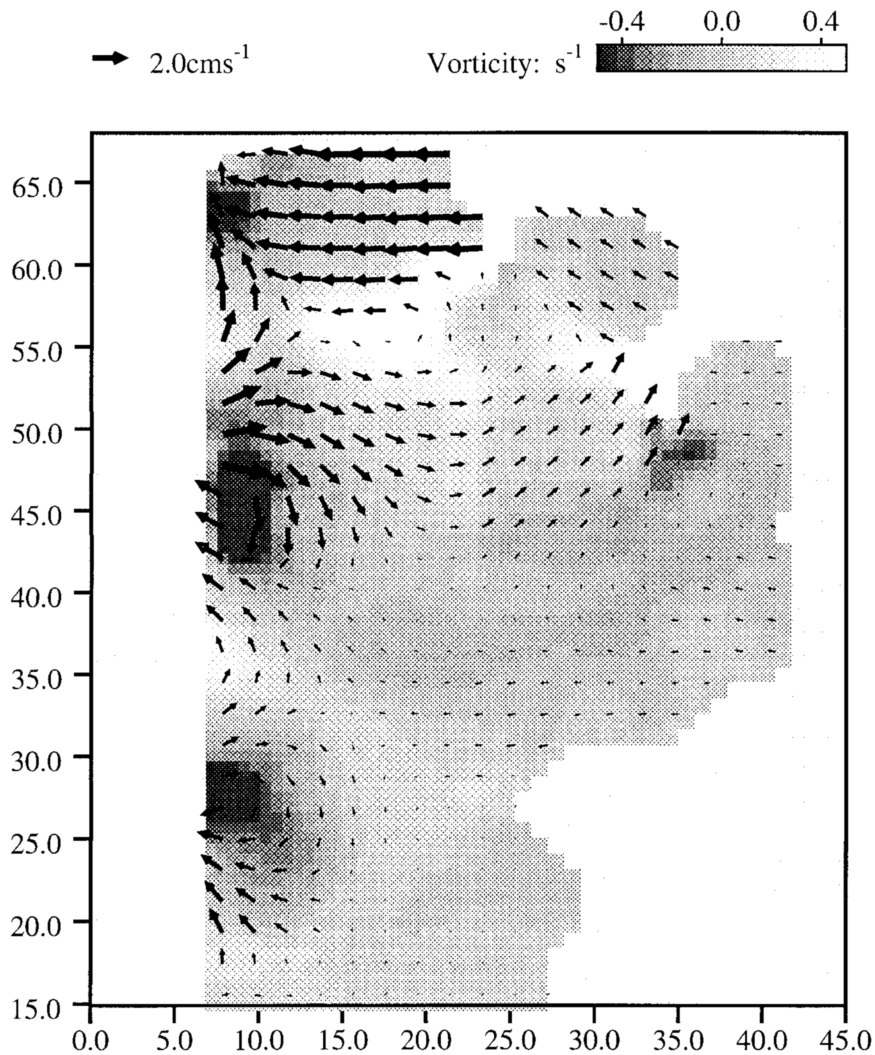

FIG. 5. Typical velocity and vorticity fields in the lower, dense overflow fluid parallel to the slope (at a height of 4 mm above the slope), calculated from particle tracking in an experiment in the square tank with a linearly stratified ambient fluid ($d_N = 6.5$ cm). The plot covers the region 15–65 cm along the slope and 0 cm (top of slope) to 45 cm down the slope. The source of dense fluid is 10 cm wide at the top of the slope (off the bottom left corner of this plot). The value of $g' = 50.9$ cm s^{-2}, $Q = 27.5$ cm^3 s^{-1}, and rotation rate of one revolution in 5.96 s.

5. Discussion and oceanographic applications

a. Overflows and eddy formation

Dense overflows on slopes can be regarded as having two main components: an inviscid alongslope geostrophic flow and a lower viscous downslope Ekman flow, which continuously drains fluid from the inviscid flow. Under certain conditions the inviscid flow can break up into a series of domes with strong cyclonic eddies in the overlying fluid. The eddies form as a result of stretching of fluid columns in the overlying fluid, which may be produced by three processes in these experiments. Two of these (initial downslope motion of the current dragging the fluid above with it and collapse due to geostrophic adjustment) are due to the initial adjustment of the flow to dynamical balance. The third process depends on stretching of the fluid column by Ekman drainage from below and can operate continuously. As discussed in LSB, this process causes a gradual downslope displacement of the inviscid current with alongslope distance because of the larger Ekman drainage from the upslope side of the current. These processes are collectively represented by the parameters Γ and Y/L.

Stratification in the ambient fluid limits the vertical extent of motions caused by the overflow. This reduces the effective height of the fluid columns, enhancing the relative stretching and thus producing stronger, more frequent eddies. As the stretching parameter (Γ_I or Γ_N) becomes larger, the frequency at which eddies are pro-

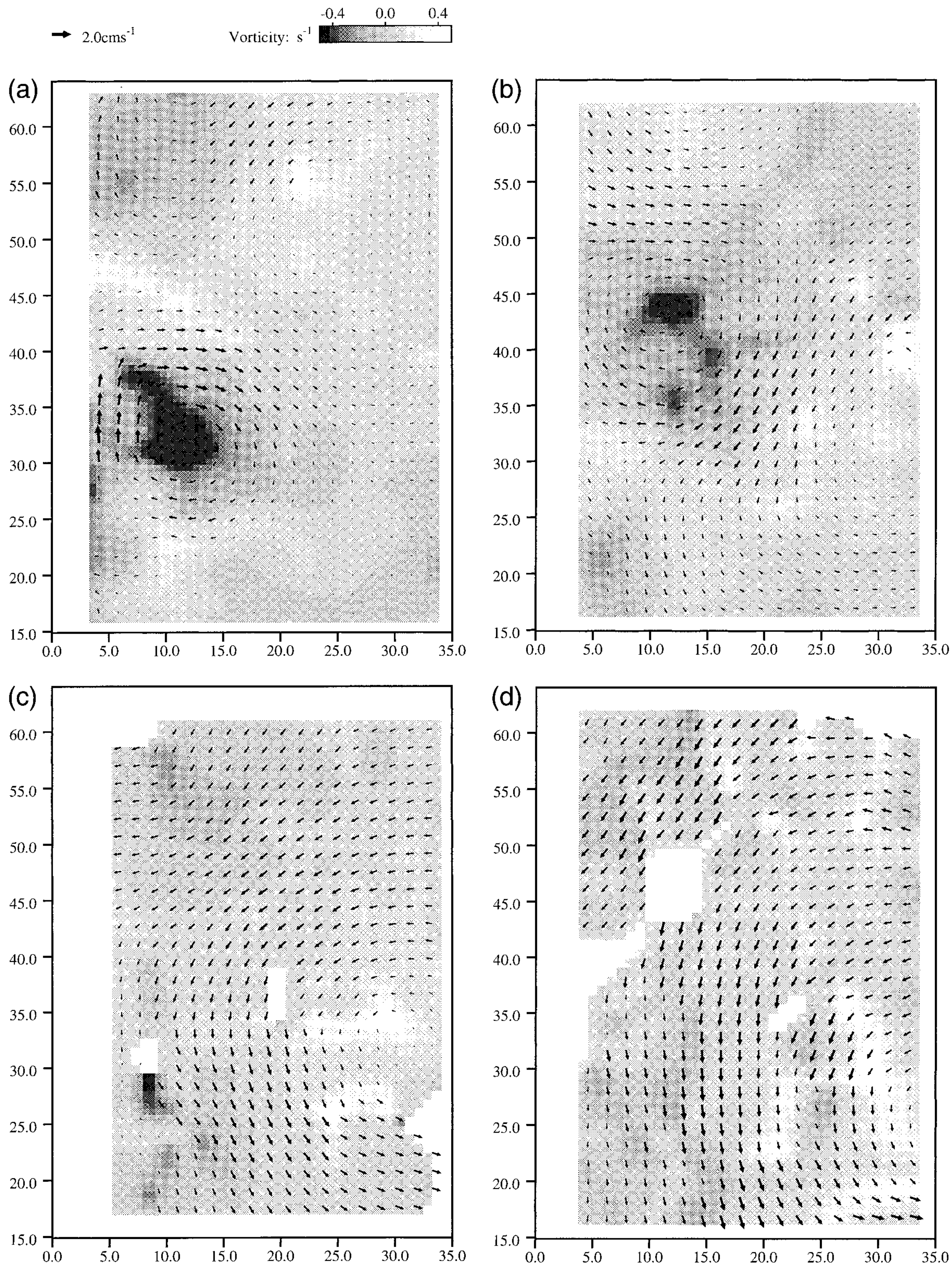

FIG. 6. Typical velocity and vorticity fields in horizontal layers (a) level with the top of the slope, (b) 5 cm, (c) 10 cm, and (d) 15 cm above this level. The parameters are similar to those in Fig. 5. The fields in this figure are all calculated from the same experiment but at different times (approximately 45 s between each), so the eddies in (a) and (b) are different.

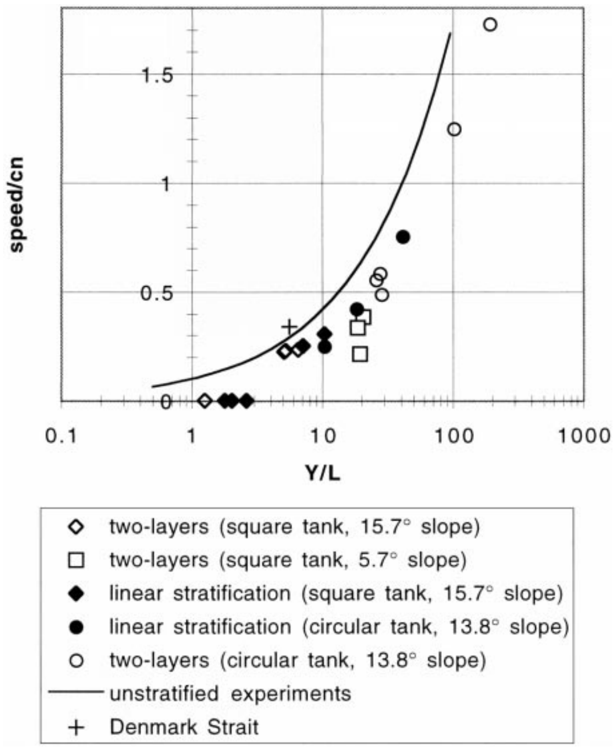

FIG. 7. The speed at which the eddy/dome structures propagate along the slope as a function of Y/L.

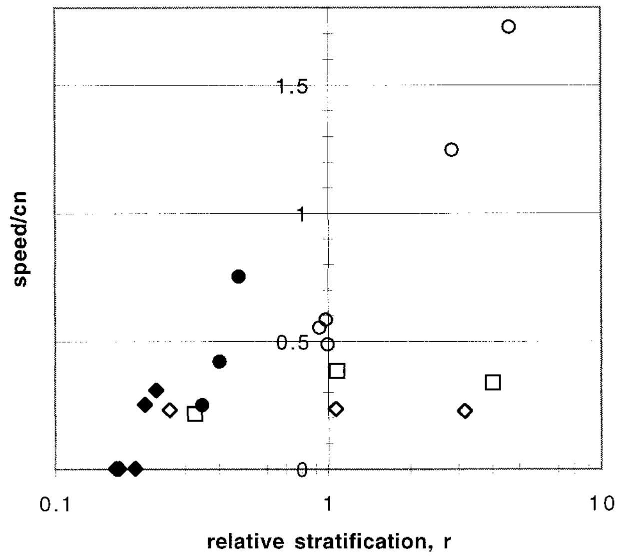

FIG. 8. The speed at which the eddy/dome structures propagate along the slope as a function of r, the relative stratification defined in Eqs. (9) and (12).

duced approaches approximately one for every two revolutions of the rotating table {equivalent to 1/(2 sin(lat)) per day on the earth}. The speed at which the eddies propagate along the slope depends on viscous effects, but this speed is observed to be slower for the stratified cases examined here than for the unstratified case. This may be due to the drag from (internal gravity) lee waves caused by flow past the cyclonic structure. The strength of the eddies was not measured directly in these experiments (except for the particle experiments), but in the unstratified experiments the relative vorticity was found to be approximately linearly related to Γ, reaching $2f$ for $\Gamma = 0.5$.

b. Examples of overflows

It is of interest to apply our results to oceanographic situations, where the only significant assumption required involves replacing the molecular viscosity of the laboratory experiments with a vertical eddy viscosity appropriate to the full-scale flows. Information about the bottom boundary layer in the deep ocean is scarce, but observations of it beneath the deep western boundary current of the North Atlantic at the Blake outer ridge by Stahr and Sanford (1999) indicate a structure that is broadly similar to that of the present experiments. Here we estimate an eddy viscosity by matching the bottom stress from a simple viscous flow to the drag based on a quadratic drag law,

$$\tau = A_Z c_N / d_A = k u^2, \tag{13}$$

where A_Z is the vertical eddy viscosity, d_A the boundary layer thickness based on this ($d_A = \sqrt{2A_Z/f}$), u is the velocity scale from the scalings in section 3, and k taken to be 2.5×10^{-3} (a typical value for oceanographic flows, e.g. Lane-Serff 1993, 1995; Bombosch and Jenkins 1995). This assumes a bulk mean flow of velocity u in the upper part of the current, with a "viscous" boundary layer of thickness d_A at the base. Equation (13) can be rearranged to give A_Z in terms of known quantities,

$$A_Z = (2k^2 u^4)/(f c_N^2) = (4k^2 Q f^2)/(g' \alpha^2). \tag{14}$$

The quantitative predictions are summarized in Table 1.

The Denmark Strait overflow is an important part of the thermohaline circulation and has been the subject of many observational and modeling programs. Dense waters formed north of Iceland flow southward through this strait, between Iceland and Greenland, and down

TABLE 1. Formulas for quantitative features of overflows given by the scalings and predicted from the experimental results.

Quantity	Symbol	Value
Rossby radius	L	$(2Qg')^{1/4-3/4}$
Nof speed	c_N	$g'\alpha/f$
Eddy viscosity	A_Z	$(4k^2Qf^2)/(g'\alpha^2)$
Draining distance	Y	$(Qf^{3/2})/(g'\alpha\sqrt{2A_Z})$
Height scale	d_N	$(2Qfg')^{1/4}N^{-1}$
Stretching parameters	Γ_I, Γ_N	$L\alpha/d_I$, $L\alpha/d_N$
Downslope displacement	X	$2.3L$
Eddy radius	a	$1.25L$
Eddy strength	w	$4\Gamma_{I\text{or}N} f$
Eddy interval (hours)	T_{int}	$(0.19/\Gamma_{I\text{or}N} + 2.4)(24/\sin(\text{lat}))$
Eddy propagation speed	c	$0.067c_N(Y/L)^{0.62}$

into the Irminger Basin in the northern North Atlantic. The observations in this region have been summarized by Dickson and Brown (1994). They show that the strength of the overflow varies on timescales of the order of days, while there is little evidence of significant variation on monthly and seasonal timescales (see also Bacon 1997). Based on these reviews and especially on the observations of Ross (1984) we take the volume flux of overflow water to be 3×10^6 m^3 s^{-1} (3 Sv: Sv $\equiv 10^6$ m^3 s^{-1}) and the density to be $\sigma = 28.0$. The density structure in the ambient seawater may be approximated by a mixed layer above a strong thermocline with a linearly stratified region below (with $N = 1.8 \times 10^{-3}$ s^{-1}). The overflow water enters at a depth of approximately 700 m with a density contrast of 0.3 ppt. The slope downstream of the strait is given by $\alpha = 0.02$ and $f = 1.3 \times 10^{-4}$ s^{-1}.

Substituting these values into our scalings we find

$$A_Z = 1.08 \text{ m}^2 \text{ s}^{-1},$$

$$L = 9.5 \text{ km},$$

$$c_N = 0.45 \text{ m s}^{-1},$$

$$Y = 51.4 \text{ km},$$

$$Y/L = 5.4,$$

$$d_N = 680 \text{ m}$$

with D slightly larger (at 700 m) and d_I smaller (at 600 m). The vertical eddy viscosity may seem very large to those more familiar with parameters appropriate in the bulk of the ocean, away from boundaries. Weatherly (1997) made measurements in a bottom boundary layer below currents of order 30 cm s^{-1}. He found friction velocities of up to $u_* = 1$ cm s^{-1}, and logarithmic bottom boundary layers of up to $d_{\ln} = 8$ m. This gives a vertical eddy viscosity (using standard turbulent boundary layer theory) of $A_Z = 0.4 d_{\ln} u_* = 0.032$ m^2 s^{-1}. Applying a similar approach as in Weatherly (1977) to the Denmark Strait (where we estimate the alongslope velocity as $u = 1.24$ m s^{-1}) gives $u_* = 6.2$ cm s^{-1}, $d_{\ln} = 28$ m, and thus $A_Z = 0.70$ m^2 s^{-1}, not very different from the result of our simpler scaling above.

Returning to our simpler scaling, this gives $\Gamma_I = 0.28$, suggesting that there is significant vortex stretching, so we expect eddy formation. From the results of the unstratified experiments we would expect that the flow would move downslope a distance $2.3L$ (21.4 km) into water approximately 1100 m deep, with an eddy radius of approximately $1.25L$ (11.9 km). The eddies should be produced with a frequency of 1/82 h, have a relative vorticity of approximately $1.1f$, and propagate at $0.19c_N$ (0.09 m s^{-1}).

Eddies have been observed above the Denmark Strait overflow (Krauss 1996; Bruce 1995). Buoys drogued at 100 m were trapped in cyclonic eddies moving southwest between the 1000-m and 1500-m isobaths (Krauss 1996). The longest record is of an eddy with a core radius of approximately 15 km. From observations near another eddy, the velocity structure is observed to decay with height, in accordance with the expected effect of the ambient stratification. The relative vorticity at the 100-m level is approximately $1.1f$. The volume transport estimated by Ross (1978) shows eight large pulses between 15 August and 15 September 1973 (this data is also shown by Bruce), and thus an interval between pulses of 93 hours. The propagation of the eddies is complicated by an overall barotropic flow to the southwest. Subtracting this flow, Krauss (1996) estimates the eddy propagation due to its own dynamics as 0.1–0.3 m s^{-1}. This is somewhat faster than our estimate, and our estimated value for Y also appears to be too small; together these both suggest that the eddy viscosity used in our model is too large.

We now apply our results to some other overflows in less detail. The Mediterranean outflow through the Strait of Gibraltar has a flux of approximately 0.7 Sv, a relative density difference of 2 ppt, and flows at a depth of 300 m onto a slope of 0.01. From Table 1, this gives $Y/L \approx 0.5$ so that in this case we expect eddies to be absent (since their presence in the experiments requires $Y/L > 1$) and viscous drainage should dominate the flow. This implies that most of the dense fluid lies in the boundary layer, with a thickness of order $(2A_z/f)^{1/2} = 40$ m. The observed Mediterranean outflow is not predominantly downslope because it is partly channeled alongslope by ridges in the bottom topography (see Fig. 5 of Baringer and Price 1998), which makes it thicker than this (about 100 m).

There are intermittent flows of up to 3 Sv through the Bass Strait (between Tasmania and Australia) carrying dense water (relative density 0.4 ppt) to the east at a depth of 100 m onto a slope of 0.14 (Baines et al. 1991). This case appears to be marginal for eddy production: $Y/L = 2.8$ and (despite the very strong stretching) the predicted time interval between eddies is longer than the typical duration of the intermittent flow (2–3 days).

In the Antarctic, ice shelf water flows into the Weddell Sea from the Filchner Depression at a depth of approximately 400 m onto a slope of 0.03. There are a number of estimates for the flux and density difference: we will take 0.5 Sv and 0.1 ppt based on the studies by Foldvik et al. (1985) and Woodgate et al. (1999). The stratification gives $d_N \approx 1$ km, so the stratification is not important in enhancing vortex stretching. With $Y/L \approx 9$ and $\Gamma \approx 0.3$ we predict eddies to be formed every 3 days and to propagate along the slope at 5 cm s^{-1}, draining downslope over a distance of order 40 km. While observations to date show variability in the flow on a range of timescales, they are not sufficiently detailed; so this prediction remains to be tested.

c. *The modeling of overflows and the oceanic bottom boundary*

The parameters for the Gibraltar outflow suggest that the flow quickly drains downslope. For this type of flow a streamtube model (e.g., Price and Baringer 1994) will provide a reasonable approximation since the mixing of properties (including momentum supplied by bottom stress) throughout the current provides a fairly accurate description of the flow. In general, however, outflows do not all follow this pattern. In applying a streamtube model to the Denmark Strait outflow (for example) one could only be confident of identifying some of the basic scales of the flow.

The observed flow development does not result from the instability of an initially two-dimensional flow. For this reason theories and models starting from a two-dimensional basic state (e.g., Swaters 1991 and 1993; Jiang and Garwood 1995) are not relevent to this particular flow (though they may be appropriate for other oceanographic flows). We demonstrated this in LSB by showing that the observed flow had no dependence on the interaction parameter μ (defined by Swaters 1991).

Jiang and Garwood (1998) construct a numerical model of an overflow on a slope and consider the effects of topographic steering. The source in their model is somewhat weaker than the Denmark Strait (0.9 Sv as opposed to 2.9 Sv) and the source fluid enters as a simple horizontal layer, despite the source being much wider than a Rossby radius. The major drawback of this model is that with a grid spacing of 4 km they do not (as they point out themselves) adequately resolve flows that scale on the Rossby radius (they estimate this to be about 5 km; our scaling gives a similar value of approximately 7 km). With both laboratory and ocean flows having flow structures on this Rossby radius scale it is clear that this numerical model is unable to resolve these significant features.

The simple isopycnic model of the Denmark Strait used by Spall and Price (1998) appears to capture many of the important features of the flow, including the formation of domes of dense fluid with cyclonic vortices in the overlying fluid. In their model eddy formation is enhanced by having an intermediate water mass flowing through the strait above the dense fluid, supplying more initially shallow upper-layer fluid than that which would otherwise be dragged into deeper water. With the dense fluid represented by a single layer, the bottom drag is distributed throughout this dense layer. This results in the domes descending (at a shallow angle) down the slope rather than moving along the slope while being drained by a viscous layer. This also means that one of the mechanisms we give for stretching columns of ambient fluid, that is, the draining of dense fluid from a dome that is maintaining its position on the slope, cannot be represented in this version of the model.

These weaknesses of the Spall and Price model are not fundamental and might be resolved by using more isopycnic layers, or by introducing a distinct bottom boundary layer (somewhat similar to a surface mixed layer). The use of such a boundary layer, added to the bottom of a conventional z-coordinate model, has been considered by Killworth and Edwards (1999). Whatever the modeling approach used, numerical models need to resolve the Rossby radius ($\sim$5 km) in order to simulate the eddy features accurately.

d. Closing remarks

Overall, our model predictions for the Denmark Strait are consistent with observations, both in terms of the basic features (such as whether eddies will be formed or not) and also in terms of detailed quantitative features (such as eddy size, location, and frequency). We have identified the significant parameters that control this type of flow so that our results can be applied to any given overflow.

A better model for the turbulent bottom boundary layer would improve the comparison still further, and more observational data such as that described by Stahr and Sanford (1999) would be useful here. The effect of the overflow on the overlying fluid in producing strong eddies and thus the possibility of strong mixing is important in the neighborhood of the overflow. The eddies also have an influence on the viscous draining flow but, in any case, all of the dense fluid will eventually drain downslope until it reaches its neutral level or the bottom of the slope. The long-term fate of the overflow water, its mixing with the ambient water, and its final injection into the water column are all controlled by the viscous draining layer.

Acknowledgments. Much of the experimental work presented here was undertaken while G.F.L.-S. was visiting DAR, supported by the Royal Society and CSIRO. G.F.L.-S. would like to thank all at DAR for their help and advice during his visit, with special thanks to David Murray for constructing the apparatus and for helping with the running of the experiments.

REFERENCES

Bacon, S., 1997: Circulation and fluxes in the North Atlantic between Greenland and Ireland. *J. Phys. Oceanogr.,* **27,** 1420–1435.

Baines, P. G., 1998: Downslope flows into stratified environment—Structure and detrainment. *Mixing and Dispersion in Stably Stratified Flows, Proceedings of the Fifth IMA Conference on Stratified Flows,* P. A. Davies, Ed., Clarendon Press, 1–21.

——, G. D. Hubbert, and S. Power, 1991: Fluid transport through Bass Strait. *Contin. Shelf Res.,* **11,** 269–293.

Baringer, M. O'N., and J. F. Price, 1997: Mixing and spreading of the Mediterranean outflow. *J. Phys. Oceanogr.,* **27,** 1654–1677.

Bombosch, A., and A. Jenkins, 1995: Modeling the formation and deposition of frazil ice beneath the Filchner–Ronne Ice Shelf. *J. Geophys. Res.,* **100,** 6983–6992.

Bruce, J. G., 1995: Eddies southwest of the Denmark Strait. *Deep-Sea Res. I,* **42,** 13–29.

Bryden, H. L., J. Candela, and T. H. Kinder, 1994: Exchange through the Strait of Gibraltar. *Progress in Oceanography,* Vol. 33, Pergamon, 201–248.

Condie, S. A., 1995: Descent of dense water masses along continental slopes. *J. Mar. Res.,* **53,** 897–928.

Dickson, R. R., and J. Brown, 1994: The production of North Atlantic Deep Water: Sources, rates and pathways. *J. Geophys. Res.,* **99,** 12 319–12 341.

Etling, D., 1997: Laboratory experiments on density currents on a slope in a rotating system. *Preprints, 11th Conf. on Atmospheric and Oceanic Fluid Dynamics,* Tacoma, WA, Amer. Meteor. Soc., 211–212.

Foldvik, A., T. Gammelsrød, and T. Tørresen, 1985: Circulation and water masses on the southern Weddell Sea shelf. *Oceanology of the Antarctic Continental Shelf,* S. S. Jacobs, Ed., Antarctic Research Series, Vol. 43, Amer. Geophys. Union, 5–20.

Jiang, L., and R. W. Garwood, 1995: A numerical study of three-dimensional dense bottom plumes on a Southern Ocean continental slope. *J. Geophys. Res.,* **100** (C9), 18 471–18 488.

——, and ——, 1998: Effects of topographic steering and ambient stratification on overflows on continental slopes: A model study. *J. Geophys. Res.,* **103** (C3), 5459–5476.

Killworth, P. D., and N. R. Edwards, 1999: A turbulent bottom boundary layer code for use in numerical ocean models. *J. Phys. Oceanogr.,* **29,** 1221–1238.

Krauss, W., 1996: A note on overflow eddies. *Deep-Sea Res. I,* **43,** 1661–1667.

Lane-Serff, G. F., 1993: On drag-limited gravity currents. *Deep-Sea Res. I,* **40,** 1699–1702.

——, 1995: On meltwater under ice-shelves. *J. Geophys. Res.,* **100,** 6961–6965.

——, and P. G. Baines, 1998: Eddy formation by dense flows on slopes in a rotating fluid. *J. Fluid Mech.,* **363,** 229–252.

Maxworthy, T., 1997: Convection into domains with open boundaries. *Annu. Rev. Fluid Mech.,* **29,** 327–371.

Nagata, Y., R. Kimura, H. Honji, Y. Yamazaki, K. Kawaguchi, and T. Hosoyamada, 1993: Laboratory experiments of dense water descending on continental slope. *Deep Ocean Circulation, Physical and Chemical Aspects,* T. Teramoto, Ed., Elsevier, 333–350.

Price, J. F., and M. O'N. Baringer, 1994: Outflows and deep water production by marginal seas. *Progress in Oceanography,* Vol. 33, Pergamon, 161–200.

Ross, C. K., 1978: Overflow variability in Denmark Strait. Report ICES CM 1978/C:21, International Council for Exploration of the Sea, Copenhagen, Denmark.

——, 1984: Temperature–salinity characteristics of the ''overflow'' water in Denmark Strait during ''Overflow 1973.'' *Rapp. Proc.-V. Reun., Cons. Perm. Int. Explor. Mer,* **185,** 111–119.

Spall, M. A., and J. F. Price, 1998: Mesoscale variability in Denmark Strait: The PV outflow hypothesis. *J. Phys. Oceanogr.,* **28,** 1598–1623.

Stahr, F. R., and T. B. Sanford, 1999: Transport and bottom boundary layer observations of the North Atlantic Deep Western Boundary Current at the Blake Outer Ridge. *Deep-Sea Res. II,* **46,** 205–243.

Swaters, G. E., 1991: On the baroclinic instability of cold-core coupled density fronts on a sloping continental shelf. *J. Fluid Mech.,* **224,** 361–382.

——, 1993: Nonlinear stability of intermediate baroclinic flow on a sloping bottom. *Proc. Roy. Soc. London,* **442A,** 249–272.

——, and G. R. Flierl, 1991: Dynamics of ventilated coherent cold core eddies on a sloping bottom. *J. Fluid Mech.,* **223,** 565–587.

Weatherly, G. L., 1977: Bottom boundary layer observations in the Florida Current. *Bottom Turbulence,* J. C. J. Nihoul, Ed., Elsevier, 237–254.

Woodgate, R. A., M. Schröder, and S. Østerhaus, 1999: Moorings from the Filchner Trough and the Ronne Ice Shelf Front: Preliminary results. FRISP Rep. 12, Alfred Wegener Institute, Bremerhaven, Germany, 6pp. [Available from Alfred Wegener Institute, Am Handelshafen 12, 27570 Bremerhaven, Germany.]

Zatsepin, A. G., V. L. Didkovskii, and A. V. Semenov, 1998: Self oscillatory mechanism of inducing a vortex structure by a stationary local source over a sloping bottom in a rotating fluid. *Oceanology,* **38,** 43–50.